The loop between helix 4 and helix 5 in the monocarboxylate transporter MCT1 is important for substrate selection and protein stability

Sandra GALIĆ*, Hans-Peter SCHNEIDER†, Angelika BRÖER*, Joachim W. DEITMER† and Stefan BRÖER*[1]

*School of Biochemistry & Molecular Biology, Australian National University, Canberra ACT 0200, Australia, and †Abteilung für Allgemeine Zoologie, FB Biologie, Universität Kaiserslautern, Postfach 3049 67653 Kaiserslautern, Germany

Transport of lactate, pyruvate and the ketone bodies acetoacetate and β-hydroxybutyrate, is mediated in most mammalian cells by members of the monocarboxylate transporter family (SLC16). A conserved signature sequence has been identified in this family, which is located in the loop between helix 4 and helix 5 and extends into helix 5. We have mutated residues in this signature sequence in the rat monocarboxylate transporter (MCT1) to elucidate the significance of this region for monocarboxylate transport. Mutation of R143 and G153 resulted in complete inactivation of the transporter. For the MCT1(G153V) mutant this was explained by a failure to reach the plasma membrane. The lack of transport activity of MCT1(R143Q) could be partially rescued by the conservative exchange R143H. The resulting mutant transporter displayed reduced stability, a decreased V_{max} of lactate transport but not of acetate transport, and an increased stereoselectivity. Mutation of K137, K141 and K142 indicated that only K142 played a significant role in the transport mechanism. Mutation of K142 to glutamine resulted in an increase of the K_m for lactate from 5 mM to 12 mM. In contrast with MCT1(R143H), MCT1(K142Q) was less stereoselective than the wild-type. A mechanism is proposed that includes all critical residues.

Key words: monocarboxylate transporter (MCT1), stereospecificity, structure–function relationship, transport mechanism.

INTRODUCTION

Transport of lactate, pyruvate and the ketone bodies, acetoacetate and β-hydroxybutyrate, is of major physiological importance in almost all cells [1]. Transport of this class of substrates is mediated by a family of monocarboxylate transporters (MCTs, human/mammalian members grouped as SLC16), members of which can be found in organisms from bacteria to man [2]. They belong to the major facilitator superfamily, which has received the transporter classification number 2.A.1.13 (see http://tcdb.ucsd.edu/tcdb/). Despite its name, the family also comprises two members that transport aromatic amino acids and thyroid hormones [2]. MCT1 appears to be the archetypical monocarboxylate transporter. It is almost ubiquitously expressed and can mediate uptake as well as release of lactate. The kinetic properties of MCT1 have been investigated in detail due to its presence in erythrocytes and cultured cell lines [3,4]. It mediates the concerted translocation of $1H^+$ and a monocarboxylate anion by an ordered mechanism in which H^+ binding precedes monocarboxylate binding [5].

The cloned MCT1 transporter has been investigated in *Xenopus laevis* oocytes [6,7]. Those studies confirmed the basic mechanism of the transporter. The hydropathy plot of the transporter indicates a classical 12 transmembrane-helix structure, with both the N- and C-terminus being located intracellularly. The membrane topology of MCT1 has been probed with peptide-specific antibodies [8]. In general, it was found that MCT1 was highly stable against proteolytic digestion in intact erythrocytes, suggesting that extracellular loops are small and not exposed [8]. It could also be demonstrated that the C-terminus has a cytoplasmic location, and that the large putatively cytoplasmic loop between helix 6 and 7 is highly sensitive to proteolytic degradation in membrane preparations, but not in intact erythrocytes. These findings confirmed the predicted two-dimensional topology of the transporter.

A number of conserved motifs and residues have been identified in the monocarboxylate transporter family [9]. The sequence motif [D/E]G[G/S][W/F][G/A]W is located in the N-terminus adjacent to transmembrane helix 1. A second motif YF-[R/K][R/K][R/L]–[N/T][G/A]–G constitutes the loop between helix 4 and 5 and the beginning of helix 5 (Figure 1). An arginine residue (R306) has been identified in helix 8 that is conserved in almost all members of the family and which is the only conserved charged residue in transmembrane regions of the MCT family. Functional analysis indicates that it is crucial for lactate binding and coupling of lactate transport to proton translocation [10]. The neighbouring aspartate (D302) cannot be replaced by other amino acids without causing complete loss of function. Substrate specificity appears to be affected by hydrophobic residues in helix 10. F360 of the rat MCT1 alters the specificity of the transporter, allowing mevalonate to be transported by MCT1 [10,11]. Conversion of two exofacial lysines to glycine in the loop between helix 7 and 8 and the loop between helix 11 and 12 (K290 and K413) renders MCT1 resistant to covalent DIDS (4,4′-di-isothiocyanostilbene-2,2′-disulphonate) modification [12], suggesting that these residues are in close proximity with the substrate translocation pore. It has also been found that monocarboxylate transport by MCT1 is sensitive to inhibition by pCMBS, whereas MCT2 is not [13,14], but the cysteine residue responsible has not been identified.

In this study we have investigated the significance of cationic and conserved amino acids in the signature sequence between helix 4 and helix 5. The results indicate that R143 and G153 are the only essential residues in this signature sequence and that movement of helix 5 during the transport cycle is essential. Analysis of the transport properties of the mutants also indicated

Abbreviations used: DIDS, 4,4′-di-isothiocyanostilbene-2,2′-disulphonate; G153V etc., mutation of amino acid Gly-153 to Val-153 etc. (for consistency, other specific amino acids are referred to by their single-letter code throughout); MCT, monocarboxylate transporter; pH_i, intracellular pH; cRNA, complementary RNA.

[1] To whom correspondence should be addressed (e-mail stefan.broeer@anu.edu.au).

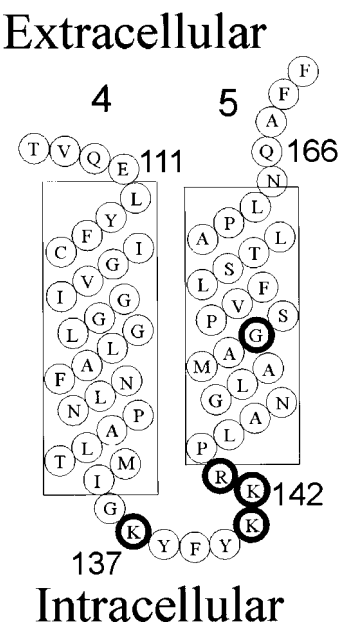

Figure 1 Predicted topology and primary sequence of transmembrane helices 4 and 5 of rat MCT1

The hydropathy plot of rat MCT1 was analysed and hydrophobic regions of sufficient length are depicted as transmembrane helices (only helix 4 and helix 5 are shown). Bold circles indicate residues that were mutated and investigated in this study. Positions of selected residues are indicated.

that the stereoselectivity is altered by mutation of residues in this loop.

MATERIALS AND METHODS

Plasmids and mutagenesis

MCT1, subcloned into oocyte expression vector pGEM-He-Juel, was used as described previously [6]. Site-directed mutagenesis was carried out using the Quick change site-directed mutagenesis kit (Stratagene, La Jolla, CA, U.S.A.) as recommended by the manufacturer. The following primers were used. Only sense primers are shown, mutated residues are shown in bold and the resulting amino acid substitutions are in parentheses):

5′-GGG TAC ACC CCC CCA **A**AT GGA GGC TGG GGC TGG-3′ (D15N)
5′-ACT ATG ATT GGC **C**AG TAT TTC TAC A-3′ (K137Q)
5′-AAG TAT TTC TAC **C**AG AAG AAG CCT TTG GCC AAT GGC-3′ (K141Q)
5′-TAT TTC TAC AAG **C**AG AGG CCT TTG GCC AAT GGC-3′ (K142Q)
5′-TC TAC AAG AAG C**A**A CCG CTA GCC AAT GGC CTG-3′ (R143Q)
5′-TTC TAC AAG AAG **AA**A CCA CTC GCG AAT GGC CTG GCT-3′ (R143K)
5′-TC TAC AAG AAG C**AC** CCG CTA GCC AAT GGC CTG-3′ (R143H)
5′-TTC TAC AAG AAG **GA**A CCG CTA GCC AAT GGC CTG-3′ (R143E)
5′-G GCC AAT GGC CTC GCG ATG GCA G**T**C AGC CCA GTG TT-3′ (G153V)
5′-C TCC GTA TTG TTC **CG**G ACG TTG ATG GA-3′ (E369R)
5′-AAG TAT TTC TAC **C**AG **C**AG CGA CCA TTG G-3′ (K141Q + K142Q)
5′-ACT ATG ATT GGC **C**AG TAT TTC TAC **C**AG **C**AG CGA CCA TTG G-3′ (K137Q + K141Q + K142Q)

Although a high-fidelity polymerase was used in these reactions, three clones were tested for transport activity for every mutant to avoid second-site mutations. Mutations were verified either by cDNA sequencing or by restriction digestion if possible (silent mutations resulting in new restriction sites are underlined).

Oocytes and microinjection

Xenopus females were obtained from the South African *Xenopus* facility (P.O. Box 480, Knysna 6570, Rep. South Africa). Oocytes (stages V and VI) were isolated by collagenase treatment (collagenase A, EC 3.4.24.3; 0.21 unit/mg; Roche, Mannheim, Germany) as described previously [15] and allowed to recover overnight.

Plasmid DNA was linearized with *Not*I and transcribed *in vitro* with T7 RNA polymerase in the presence of the cap analogue P1-5′-(7-methyl)-guanosine-P3-5′-guanosinetriphosphate (m^7G(5′)ppp(5′)G (Invitrogen, Groningen, The Netherlands) with the T7-mMessage mMachine Kit according to the protocol of the manufacturer (Ambion, Austin, Texas, U.S.A.). Oocytes were microinjected with 10 nl of wild-type or mutated rat MCT1 cRNA (complementary RNA) in water at a concentration of 1 μg/μl, by using a microinjection device (WPI Instruments, Sarasota, Florida, U.S.A.).

Recording of intracellular pH (pH_i) values

Double-barrelled pH-sensitive microelectrodes to measure pH_i and membrane potential, were prepared as described previously [7,16]. Briefly, the electrodes were pulled in two stages and silanized by placing a drop of 5% tri-*N*-butylchlorosilane in 99.9% pure carbon tetrachloride to fill the prospective ion-selective barrel and then baking the pipette on a hot plate at 475 °C for 4.5–5 min.

For pH-selective microelectrodes a small amount of H^+ cocktail (Fluka 95291) was backfilled into the tip of the silanized barrel and the remainder filled with 0.1 M sodium citrate, pH 6.0 (titrated with HCl). The reference barrel was filled with 3 M KCl. Electrodes were accepted for experiments if their response exceeded 50 mV per unit change in pH; on average they responded with a change of 54 mV to a change in pH by one unit. The central and the reference barrels were connected by chlorided silver wires to the headstages of an electrometer amplifier.

Flux measurements

For each determination, groups of seven cRNA- or non-injected oocytes were washed twice with 4 ml of ND96 buffer (96 mM NaCl, 2 mM KCl, 1 mM $MgCl_2$, 1.8 mM $CaCl_2$, and 5 mM Hepes, titrated with NaOH to pH 7.0 unless stated otherwise) before incubation at 23 °C in a 5 ml polypropylene tube containing 70 μl of the same buffer supplemented with 5 kBq L-[U-^{14}C] lactate (5.62 GBq/mmol) or [1,2–^{14}C]acetate (1.85 GBq/mmol; both radiochemicals were supplied by Amersham Biosciences, Castle Hill, NSW, Australia) and different amounts of unlabelled substrate. Transport was stopped after different time intervals by washing oocytes three times with 4 ml ice-cold ND96 buffer. Repeated washing steps did not result in leakage of labelled lactate (results not shown). Single oocytes were placed into scintillation vials and lysed by addition of 200 μl of 10% SDS. After lysis, 3 ml of scintillation fluid was added, and the radioactivity was determined by liquid scintillation counting. For efflux, oocytes were incubated in ice-cold buffer during injection of 50 nl of

a mixture of equal volumes of carrier-free L-[U-^{14}C]lactate and 200 mM lactate. Efflux was initiated by washing oocytes twice with 4 ml of ND96 buffer at 23 °C. Oocytes were subsequently suspended in 1ml ND96 and aliquots of 100 μl were removed for liquid scintillation counting.

Membrane preparation, surface biotinylation and Western blotting

For preparation of membranes, 15 oocytes were homogenized in 1.1 ml of homogenization buffer [50 mM Tris/HCl, 10 mM NaCl, 1 mM EDTA, 1 mM Pefabloc (Roche, Mannheim, Germany) and titrated with HCl to pH 7.5] by trituration using a tip (1 ml) of an automatic pipette. The homogenate was subsequently centrifuged at 2000 **g** for 10 min at 4 °C to remove cell debris. The supernatant (1 ml) was transferred to a microcentrifuge tube and was centrifuged for 30 min at 140000 **g** at 4 °C to separate out the membranes. The pellet was dissolved in SDS sample buffer and subjected to SDS/PAGE (12 % gel).

To determine plasma membrane expression, 15 oocytes were washed three times with 4 ml of ice-cold PBS, pH 8.0. Subsequently oocytes were incubated in 0.5 ml of sulpho-NHS-lc-Biotin (0.5 mg/ml; Pierce, Rockford, U.S.A.) solution in PBS for 10 min at 23 °C. The reagent was removed by washing oocytes four times with 4 ml of ice-cold PBS, pH 8.0. Subsequently oocytes were lysed by incubation in 1 ml of lysis buffer (150 mM NaCl, 20 mM Tris/HCl, pH 7.5, and 1 % Triton X-100) for 30 min on ice. The lysate was centrifuged at top speed in a tabletop centrifuge for 15 min at 4 °C and the supernatant was mixed with 30 μl of Streptavidin-coated agarose particles (Pierce, Rockford, U.S.A.). The suspension was incubated at 4 °C overnight with slight agitation. Agarose particles were washed four times with 1 ml of lysis buffer and the pellet subsequently resuspended in 10 μl of SDS/PAGE sample buffer. Samples were boiled for 5 min and an aliquot of 30 μl of each was loaded on to the gel.

After gel electrophoresis, proteins were blotted onto nitrocellulose membranes. MCT1 was detected using an anti-peptide antibody at a 1:4000 dilution that was raised against a mouse MCT1 peptide and which has been characterized previously [17]. Antibody binding was detected by enhanced chemiluminescence using the ECL® system, according to the manufacturers instructions, using the provided secondary antibody at a dilution of 1:5000 (Amersham Biosciences).

Data analysis

For the determination of kinetic parameters, non-linear regression algorithms of Microcal Origin software (Microcal Software, Inc.; Northampton, U.S.A.) were used. When using pH-sensitive microelectrodes, single oocytes were superfused with complete sets of substrate concentrations. Initial slopes of pH responses to substrate addition were used to calculate K_m and V_{max} for individual oocytes. These were subsequently averaged to determine the final mean $K_m \pm$ S.D. from several oocytes (number of oocytes indicated by n). For radioactive-flux measurements each individual datapoint represents the difference between the mean $\pm$ S.D. uptake activity of n expressing and n non-injected oocytes (usually $n = 7$). The S.D. of the difference was calculated by Gauss' law of error propagation [18].

RESULTS

The loop between helix 4 and helix 5 contains three lysine residues and one arginine residue. Among these residues K141, K142 and R143 are well-conserved in most members of the MCT family. The only other well-conserved residue close to this loop is G153 in helix 5 (Figure 1).

Table 1 Transport properties of MCT1 mutants

Summary of kinetic constants determined for MCT1 mutants after expression in *Xenopus* oocytes. All kinetic constants were derived from transport experiments using L-[^{14}C]lactate. Surface expression and V_{max} were determined after 4 days of expression.

Expressed cDNA	L-lactate K_m (mM)	Vmax (pmol/min per oocyte)	Relative surface expression
MCT1	5 ± 1	255 ± 24	1
D15N	2.9 ± 0.6	80 ± 5	0.54
K137Q	8 ± 3	228 ± 31	0.92
K141Q	4 ± 1	196 ± 24	1.15
K142Q	12 ± 2	267 ± 24	1.09
K141Q/K142Q	10 ± 2	228 ± 31	0.87
K137Q/K141Q/K142Q	14 ± 4	452 ± 56	0.81
R143Q	–	Not detectable	0.59
R143K	–	Not detectable	0.77
R143H	5 ± 1	109 ± 10	0.78
G153V	–	Not detectable	Not detectable
E369R	–	Not detectable	0.33

To test the significance of the loop between helix 4 and helix 5 and the beginning of helix 5, the following mutants were generated: K137Q, K141Q, K142Q, R143Q and G153V. As a first screening, all mutated cDNAs were injected into *Xenopus* oocytes and the kinetic constants of lactate transport were compared with those of the wild-type (Table 1). Of the five residues only R143 and G153 were essential for transport. Transport activity of R143Q and G153V was too low to be evaluated. In oocytes expressing an R306Q mutant, which we have analysed previously [10], proton transport was still detectable at high extracellular lactate concentration, although uptake of labelled lactate was not significantly higher than in non-injected oocytes. However, neither R143Q- nor G153V-expressing oocytes displayed significant changes in pH_i upon superfusion with lactate or pyruvate at high concentration (Figure 2). It was noted in some experiments that G153V-expressing oocytes had a more alkaline resting pH but, in other experiments, pH_i was similar to non-injected oocytes. All mutants were translated in significant amounts in *Xenopus* oocytes (Figure 3). Surface biotinylation experiments revealed that plasma-membrane expression of R143Q was significantly reduced compared with the wild-type, whereas G153V was undetectable in the plasma membrane (Figure 4 and Table 1).

The kinetic constants of mutant transporters K137Q and K141Q were similar to those of the wild-type (Table 1), however, it was noticed that K142Q displayed a significantly higher K_m value than the wild-type (12 ± 2 mM vs 5 ± 1 mM; Figure 5A). The pH-dependence of lactate transport remained unchanged in all three mutants (Figure 6), indicating that proton binding and the associated increase of lactate affinity was not disturbed. The loop between helix 4 and helix 5 is localized on the cytosolic side of the membrane. To test whether kinetic parameters might have changed more dramatically on the inside, we determined the extent of trans-stimulation of lactate uptake by preloading oocytes for 20 min with 20 mM lactate. The extent of trans-stimulation in the mutants, however, was similar to that observed in the wild-type (Table 2). In agreement with an increased K_m for lactate we found that efflux of preloaded lactate was slightly decreased in the mutant (Figure 5B). When analysed as a first order reaction, the efflux rate constant was reduced from 0.09 ± 0.02 min^{-1}

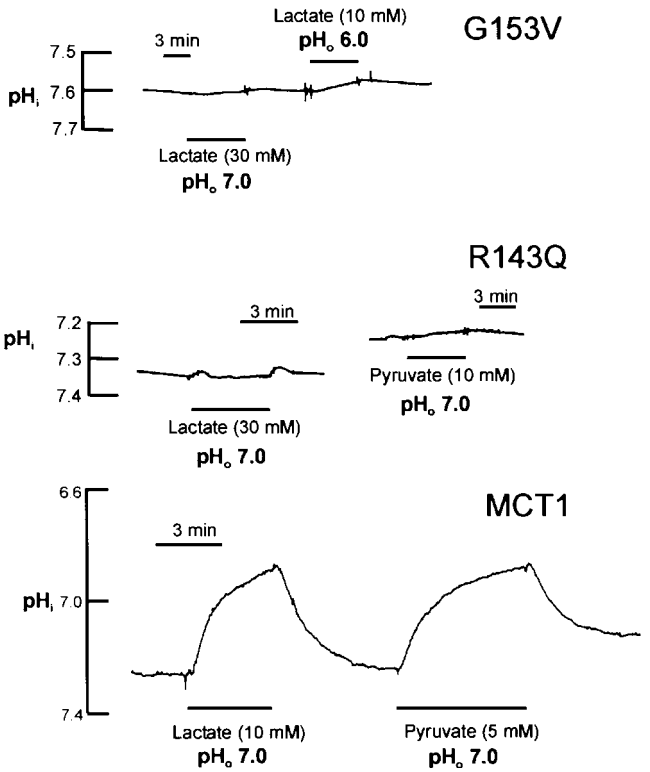

Figure 2 Changes in the cytosolic pH elicited by superfusion of oocytes expressing MCT1, mutant G153V or mutant R143Q with substrate-containing or substrate-free solutions

Each oocyte was injected with 10 ng cRNA encoding mutant or wild-type MCT1. Transport activity was recorded after an expression period of 4–7 days. Superfusion of oocytes expressing MCT1(G153V) with 30 mM L-lactate (pH 7.0) or 10 mM L-lactate (pH 6.0) did not cause significant changes in the cytosolic pH. Similarly, superfusion of MCT1(R143Q) expressing oocytes with 30 mM L-lactate (pH 7.0) or 10 mM pyruvate (pH 7.0) did not elicit any changes in the cytosolic pH. The cytosolic pH of MCT1 expressing oocytes, by contrast, reacted immediately to lactate- or pyruvate-containing solutions. Superfusion intervals are indicated by bars. pH_o, extracellular pH.

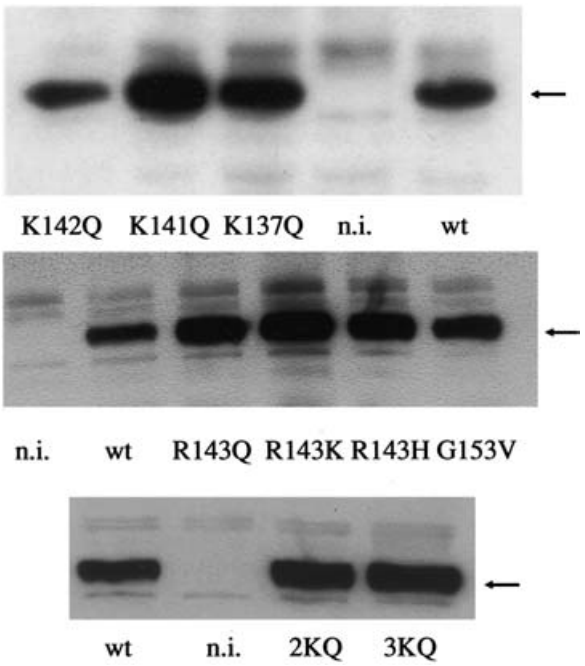

Figure 3 Detection of MCT1 in membrane preparations of *Xenopus* oocytes

Oocytes were each injected with 10 ng cRNA encoding wild-type (wt) or mutated MCT1 (mutation as indicated) or remained uninjected (n.i.). After an expression period of 4–6 days 15 oocytes were homogenized and membranes were isolated by high-speed centrifugation. Pellets were dissolved in SDS sample buffer and proteins separated by SDS polyacrylamide gel electrophoresis. Proteins were transferred onto nitrocellulose membranes and detected with anti-peptide antibodies. Apart from the major MCT1-specific band (arrow), the antibody also recognised other proteins, which were present in non-injected oocytes and thus have to be considered non-specific. 2KQ, double mutant K141Q + K142Q; 3KQ, triple mutant K137Q + K141Q + K142Q.

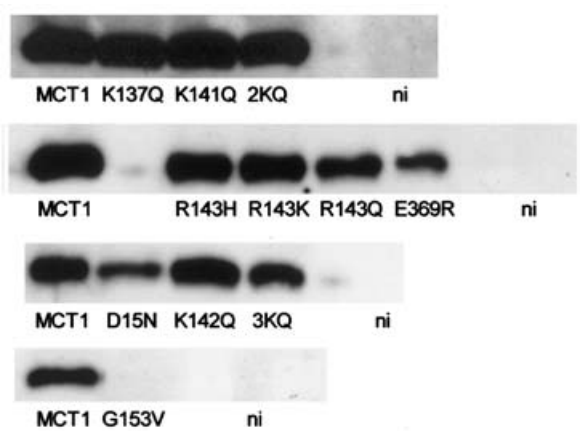

Figure 4 Expression of MCT1 mutants in the plasma membrane

Oocytes were each injected with 10 ng cRNA encoding wild-type (MCT1) or mutated MCT1 (mutation as indicated) or remained uninjected (ni). After an expression period of 4 days groups of 14 oocytes were incubated with biotin-conjugated succinimide ester to label surface-exposed lysine residues. Subsequently, oocytes were lysed and biotinylated protein was bound to streptavidin–agarose. The biotinylated proteins were separated by SDS/PAGE and MCT1 was detected after Western blotting using a MCT1-specific antibody. 2KQ, double mutant K141Q + K142Q; 3KQ, triple mutant K137Q + K141Q + K142Q. Samples from non-injected (ni) oocytes are separated by an empty lane from samples of MCT1-expressing oocytes.

to 0.07 ± 0.02 min^{-1}. In agreement with the observed transport activities, similar amounts of the K137, K141 and K142Q proteins were produced (Figure 3) and expressed at the plasma membrane (Figure 4) as wild-type MCT1.

The increase of the K_m value in the K142Q mutant indicated a possible involvement of this residue in substrate recognition. As K142Q is very close in the primary structure to K141 and K137, we wondered whether a combined mutation of all three residues might result in a more conspicuous phenotype. Both the double mutant K141Q/K142Q (2KQ in Figures 3 and 4) and the triple mutant K137Q/K141Q/K142Q (3KQ in Figures 3 and 4) had transport activities that matched, or even exceeded, that of the wild-type and were expressed in the membrane (Table 1 and Figures 3 and 4). The affinity of lactate for the mutated transporter remained decreased. For the double mutant K141Q/K142Q and the triple-mutant K137Q/K141Q/K142Q, K_m values of 10 ± 3 mM and 14 ± 3 mM respectively were determined. These results suggested that K142 was the major determinant for the shift of the K_m. The increase of the K_m value in the triple-mutant was compensated for by an increase in the V_{max}, although surface expression was less than that of the wild-type (Figure 4).

The K_m of L-lactate in the K142Q mutant was close to the K_m of D-lactate for the MCT1 wild-type transporter. Thus we analysed whether mutation of K142 might have an effect on stereoselectivity by determining the K_m of D- and L-lactate transport in the K142Q mutant and in the wild-type (Table 3). Although stereoselectivity was not lost in the mutant we found

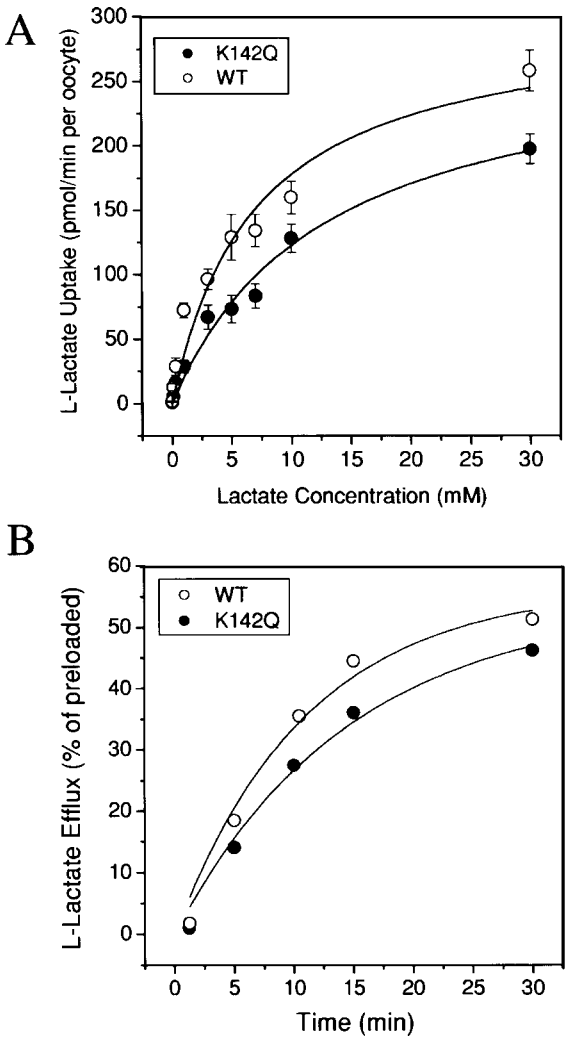

Figure 5 Analysis of L-[^{14}C]lactate uptake and efflux in MCT1(K142Q) expressing oocytes

Oocytes were each injected with 10 ng cRNA encoding wild-type (WT) or mutated MCT1 (K142Q) or remained uninjected. After an expression period of 4–7 days uptake of L-lactate was analysed at different concentrations to determine kinetic constants (see Table 1) of lactate transport (**A**). The transport activity of non-injected oocytes is already subtracted. For lactate efflux (**B**) oocytes were injected in ice-cold buffer with 50 nl L-[^{14}C]lactate plus unlabelled lactate at a final concentration of 100 mM. Efflux was initiated by washing oocytes with buffer at ambient temperature. Samples were taken from the supernatant of 7 oocytes. As a result, standard deviations cannot be presented. The efflux activity was similar in two different oocyte batches.

that the ratio of the K_m values of D- over L-lactate dropped from approx. 3-fold to 2-fold.

The R143Q mutant could not be characterized because of its low activity. To rescue the mutant we generated conservative replacements by lysine and histidine. The R143K mutant did not show any activity, the R143H mutant, however, had transport activities ranging between 5% to 58% of that of the wild-type. The large deviation of transport activities between different clones of the same mutation was unusual and was thus investigated further. It has been reported that mutations resulting in trafficking defects can be partially overcome by increasing the amount of injected RNA [19]. Increasing the amount of injected cRNA from 10 ng to 20 ng resulted in a 24% increase of the transport activity in MCT1 wild-type-expressing oocytes, suggesting that protein synthesis and/or trafficking is largely saturated by injection of

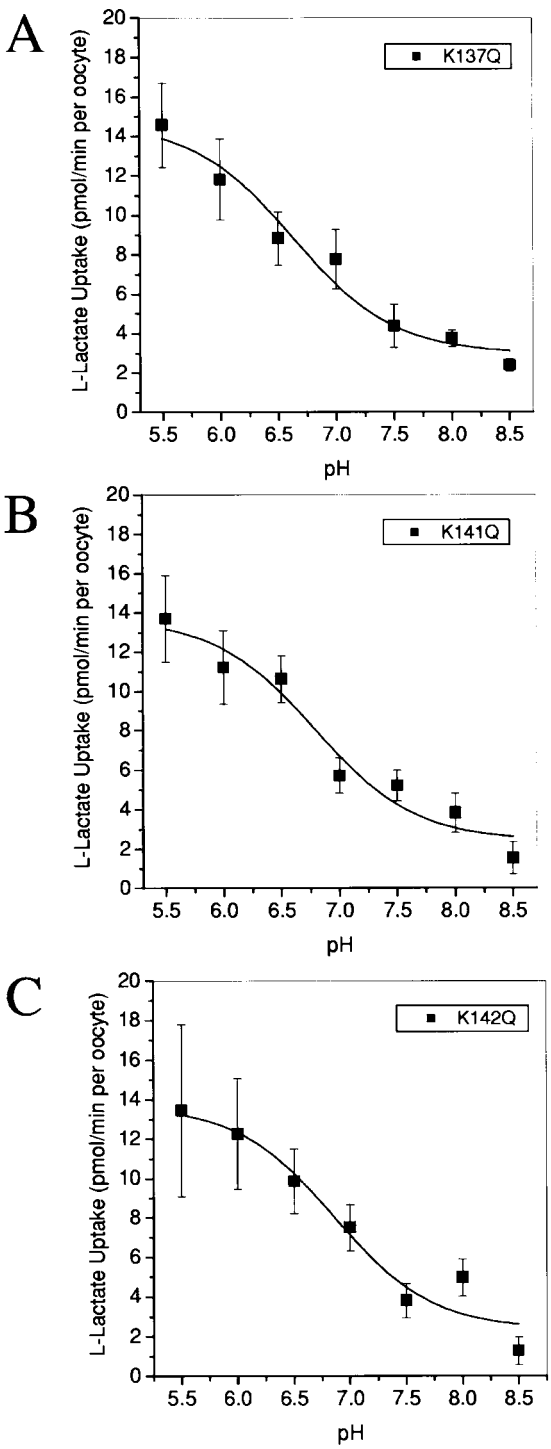

Figure 6 pH dependence of lactate transport in MCT1 mutants

Oocytes were each injected with 10 ng cRNA encoding MCT1 mutants (K137Q, K141Q, K142Q) or remained uninjected. After an expression period of 4–6 days uptake of L-[^{14}C]lactate (100 μM) was determined at different pH over a time period of 7 min. The transport activity of non-injected oocytes has been subtracted.

10 ng MCT1 cRNA. For the three individual clones of the R143H mutation, however, stimulation of lactate uptake activity by 70%, 266% and 110% was observed, supporting the notion of a trafficking problem. In further support of a role for this residue in protein trafficking we found different levels of surface expression

Table 2 Trans-stimulation of wild-type and mutant MCTs

Oocytes were injected with 10 ng cRNA encoding wild-type or mutated MCT1. After an expression period of 4 days uptake of L-[U-^{14}C]lactate (100 μM) was determined over a period of 5 min before and after preloading of oocytes with 20 mM L-lactate for 20 min.

	L-Lactate uptake (pmol/5 min per oocyte)		
Clone	Before preloading	After preloading	Stimulation (%)
MCT1	9.2 ± 1.6	13.4 ± 2.6	150
MCT1(K137Q)	5.2 ± 1.6	12 ± 2.4	219
MCT1(K141Q)	7.8 ± 1.6	14.4 ± 2.8	185
MCT1(K142Q)	7 ± 1.8	12 ± 1.4	171

Table 3 Stereoselectivity of MCT1 and the K142Q mutant

MCT1 wild-type and the mutant K142Q were expressed in oocytes. After 4–5 days expression, oocytes were superfused with different concentrations of D-lactate and the substrate-induced changes of the intracellular pH were recorded by pH-sensitive microelectrodes. K_m values are given in [mM]. K_m values for L-lactate were taken from Table 1 and were derived from flux studies using L-[^{14}C]lactate.

	MCT1	K142Q	R143H
K_m L-lactate	5 ± 1 (Table 1)	12 ± 2 (Table 1)	5 ± 1 (Table 1)
K_m D-lactate	16 ± 6 (n = 10)	26 ± 14 (n = 9)	24 ± 4 (n = 10)
Ratio D/L	3.2	2.2	4.8

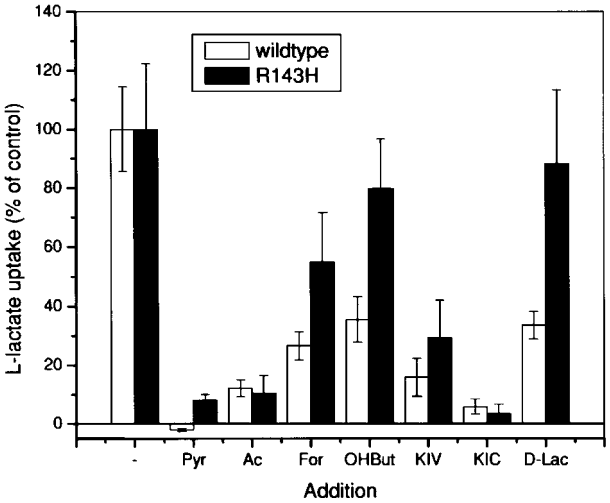

Figure 7 Inhibition of L-lactate uptake by other monocarboxylates in MCT1(R143H) expressing oocytes

Oocytes were each injected with 10 ng cRNA encoding wild-type MCT1 or MCT1(R143H) or remained uninjected. After an expression period of 4 days, uptake of 100 μM L-[^{14}C]lactate was determined in the presence or absence of 10 mM pyruvate (Pyr), acetate (Ac), formate (For), D,L-2-hydroxybutyrate (OHBut), ketoisocaproate (KIC, 2-oxoisohexanoate), ketoisovalerate (KIV, 2-oxoisovalerate) or D-lactate (D-Lac). The transport activity in the presence of different monocarboxylates is given as % control activity. Control transport in the wild-type was 69 ± 10 pmol/5 min per oocyte and 24 ± 5 pmol/5 min per oocyte in the R143H mutant.

Table 4 Changes in cytosolic pH induced by different substrates in oocytes expressing MCT1 or its mutant R143H

MCT1 wild-type and the mutant R143H were expressed in oocytes. After 4 days expression, each oocyte was superfused with 10 mM each of L-lactate, D-lactate, acetate, formate, pyruvate and D,L-hydroxybutyrate and the substrate-induced changes of the intracellular pH were recorded by pH-sensitive microelectrodes. Initial pH changes are given relative to that induced by 10 mM L-lactate in each group to compensate for differences between individual oocytes (n = 5 in both groups).

Substrate (10 mM)	MCT1	R143H
L-Lactate	1	1
D-Lactate	0.69 ± 0.07	0.45 ± 0.05
Acetate	0.88 ± 0.13	1.0 ± 0.2
Formate	0.24 ± 0.08	0.06 ± 0.04
Pyruvate	0.85 ± 0.25	0.82 ± 0.07
D,L-Hydroxybutyrate	0.46 ± 0.11	0.35 ± 0.1

associated with the different substitutions in R143 (Figure 4). The lowest surface expression was observed in the inactive R143Q mutant.

Expression of wild-type MCT1 in *Xenopus* oocytes is very stable. After an increase in the transport activity over the first 4 days, no decline was observed over the next 3–4 days. The transport activity of the R143H mutant, compared with the wild-type, reached 19% on day 3, increased to 39% on day 4 but subsequently declined to 26% on day 5 and 20% on days 6 and 7. Thus, it appears that in oocytes the R143H mutant is less stable than the wild-type.

The partial rescue of the transport defect in the R143H mutant allowed a kinetic analysis of the mutant. For lactate, a K_m of 5 ± 1 mM was determined, which was identical to that of the wild-type. To investigate the substrate specificity of the R143H mutant we determined lactate uptake (0.1 mM) in the presence of an excess of unlabelled monocarboxylates (10 mM) (Figure 7). A comparison of the inhibition pattern of the mutant with the wild-type revealed that most monocarboxylates inhibited the mutant less strongly than the wild-type with the notable exception of pyruvate, acetate and 2-ketoisocaproate. The change of substrate specificity was confirmed by measuring initial pH changes induced by MCT1 substrates (Table 4). To compensate for the different maximum velocities in both groups, the acidification induced by 10 mM L-lactate was set to 1 and pH changes elicited by other substrates were compared with it. Cytosolic acidification induced by formate, D,L-hydroxybutyrate and D-lactate was significantly slower in MCT1(R143H)-expressing oocytes when compared with the pH change induced by the same substrates in MCT1-expressing oocytes. Acidification induced by acetate and pyruvate, on the other hand, were similar in both groups (Table 4). The differences in the selectivity between L- and D-lactate suggested a change in stereospecificity in the R143H mutant. An increase in stereospecificity was confirmed by determination of the K_m value for D-lactate, which increased from 16 ± 6 mM in the wild-type to 24 ± 4 mM in the mutant (Table 3), whereas the K_m for L-lactate remained unaltered.

We also determined kinetic constants of acetate transport, which appeared unaffected by the mutation. In agreement with the competition experiments, K_m values of acetate transport of 1.6 ± 0.4 mM and 2 ± 0.6 mM were determined for the wild-type and the mutant, respectively (Figure 8A). Surprisingly, V_{max} of acetate transport was the same in the mutant and in the wild-type, whereas the V_{max} of lactate transport in the mutant never exceeded 40% of the maximum velocity of the wild-type (Figure 8B). These results suggested that the mutation R143H affects both protein stability and kinetic properties of the transporter.

The lack of stability of the R143H mutant raised the possibility that this residue might form a charge pair with a negatively charged residue in the protein, thus stabilizing its structure. The only

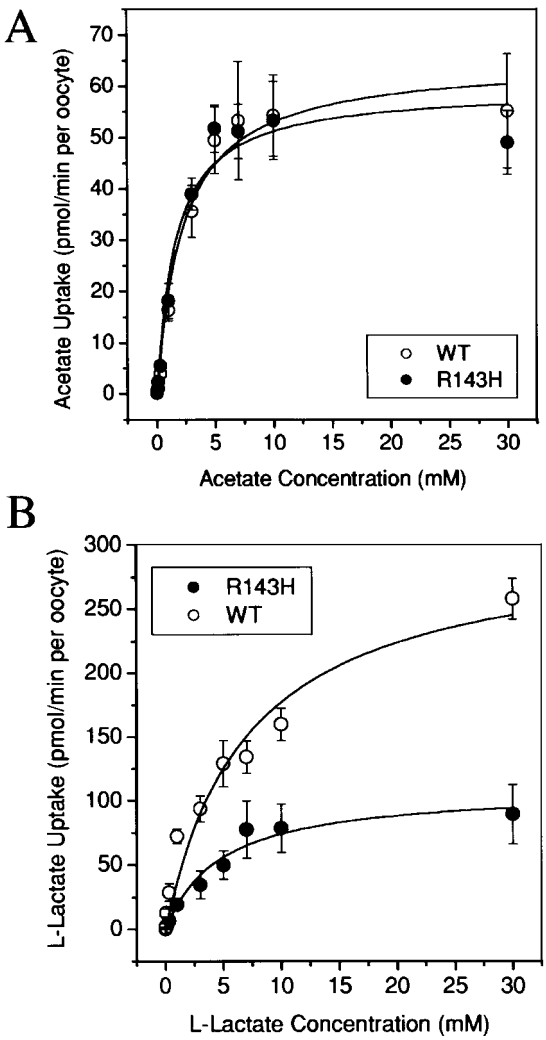

Figure 8 Kinetic parameters of L-lactate and acetate transport in MCT1 and MCT1(R143H)

Oocytes were injected with 10 ng cRNA encoding wild-type MCT1 (WT) or MCT1(R143H) or remained uninjected. After an expression period of 4 days, uptake of [^{14}C]acetate (**A**) or L-[^{14}C]lactate (**B**) was determined at concentrations ranging from 0.1 to 30 mM. The transport activity of non-injected oocytes was subtracted. The V_{max} of lactate transport in the R143H mutant (●) was significantly reduced compared with the wild-type (○). No significant difference was observed for the V_{max} of acetate transport between oocytes expressing MCT1(R143H) (●) or wild-type MCT1(○).

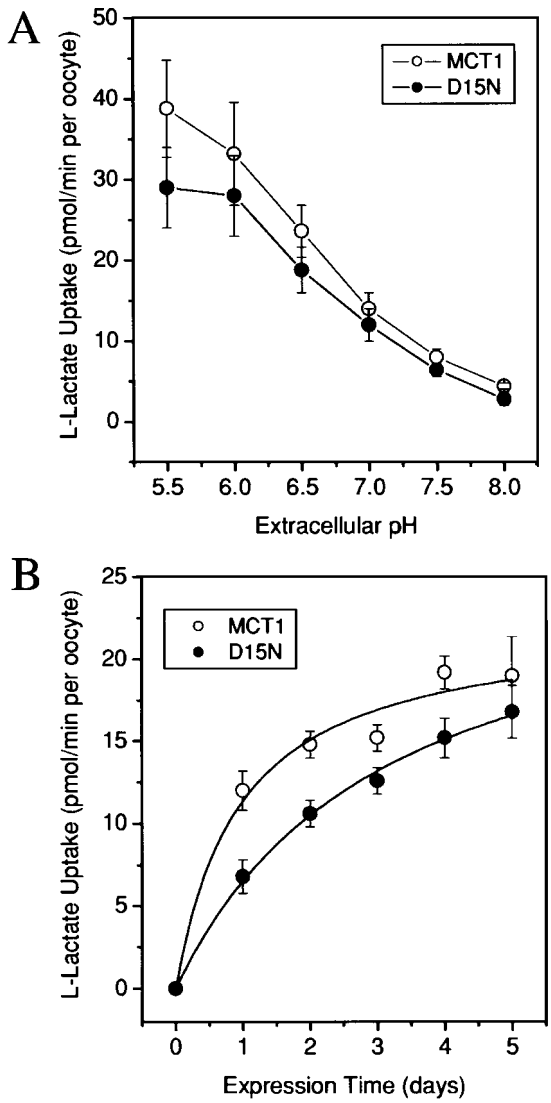

Figure 9 Characteristics of MCT1(D15N)

Oocytes were injected with 10 ng cRNA encoding wild-type MCT1(○) or MCT1(D15N) (●) or remained uninjected. (**A**) After an expression period of 5 days, uptake of L-[^{14}C]lactate (100 μM) was determined at different pH in both groups of oocytes. The transport activity of non-injected oocytes was subtracted. (**B**) Lactate uptake activity (100 μM) was determined daily throughout the expression to compare the increase of surface expression in oocytes expressing wild-type MCT1 with oocytes expressing MCT1(D15N).

two residues that have a suitable position in the proposed secondary structure of MCT1 are the highly conserved residue D15 at the entry of helix 1 and E369 at the end of helix 10. The mutant D15N had a similar K_m and pH dependence as the wild-type (Table 1 and Figure 9A), suggesting that D15 was unlikely to form a charge pair with R143 or to participate in proton transport. However, D15N had a significantly reduced V_{max} after 4 days of expression (Table 1) and there was a notable delay in expression when transport activity was recorded over a period of 5 days after injection, suggesting a trafficking defect (Figure 9B). The delayed expression was paralleled by a significantly reduced surface expression of the D15N mutant (Figure 4). Mutation of E369R, on the other hand, resulted in an inactive transporter (Figure 10A). Significant amounts of the protein were produced (Figure 10B), but surface expression was much lower than that of the wild-type (Figure 4). The double mutant R143E/E369R was found to be inactive as well, although significantly more protein was produced (Figures 10A and 10B). The low-level of expression observed in the R143E mutant further supports the involvement of R143 in protein stability and/or folding.

In summary it appears that the signature motif between helix 4 and helix 5 is involved in several functions, such as conformational movements, protein stability, trafficking and stereoselectivity. However, it is unlikely to directly participate in substrate translocation.

DISCUSSION

In this study we have analysed the significance of a conserved signature sequence that is found in members of the SLC16

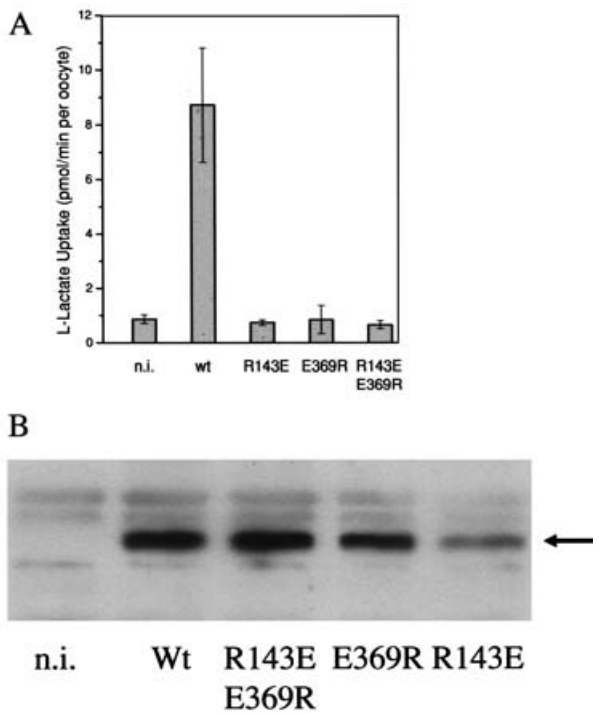

Figure 10 Mutation of residues considered to be candidates of ion-pair formation in MCT1

Oocytes were injected with 10 ng cRNA encoding wild-type (wt) or mutated MCT1 (mutation as specified) or remained uninjected (n.i.). After an expression period of 4–6 days L-[^{14}C]lactate uptake activity was determined over an incubation period of 5 min (**A**). From the same batch, 15 oocytes were homogenized and membrane proteins were isolated for Western blotting (**B**). Proteins were transferred onto nitrocellulose membranes and detected with anti-peptide antibodies. Apart from the major MCT1-specific band (arrow), the antibody also recognised other proteins, which were present in non-injected oocytes and thus have to be considered non-specific.

family of monocarboxylate transporters and constitutes the loop between helix 4 and helix 5 and the beginning of helix 5: YF-[R/K][R/K][R/L]–[N/T][G/A]–G [1]. Given that MCT1 is an anion–proton cotransporter we focused our attention on the analysis of the positively charged residues in the conserved loop between helix 4 and helix 5 and the highly conserved glycine residue at the end of the motif. Of the residues tested in this loop only two were found to be essential for transport function, namely R143 and G153.

Glycine residues in transmembrane helices are generally thought to provide flexibility, because of the freedom of rotation of the Ψ and φ bonds in the peptide backbone [20]. Replacement of glycine by a bulkier residue limits the flexibility causing the helix to become more rigid. It is tempting to speculate that G153, which is located halfway through the membrane in helix 5, has such a function and that mutation of this residue renders the helix inflexible. An alternative explanation, particularly for the striking absence of the G153V mutant from the plasma membrane, is an involvement of helix 5 in interactions with the trafficking subunit CD147 that some monocarboxylate transporters require for surface expression [21].

The second essential residue in this sequence is R143. The only conservative replacement that resulted in a partial rescue of the activity was R143H, whereas both R143K and R143Q remained inactive. Our results indicate several functions for residue R143. Four observations indicate a role in protein stability and trafficking: (i) expression levels of the R143H transporter varied widely between different concentrations of cRNA, (ii) activity of the transporter decreased relative to the wild-type after the fourth day of expression, which is rather unusual for expression in *Xenopus* oocytes (results not shown), (iii) expression levels increased significantly by increasing the amount of injected RNA, which is an indicator of trafficking mutants ([19] and results not shown), and (iv) replacement of R143 by glutamine, lysine or histidine resulted in different levels of surface expression.

Ion pairs are known to play a role in helix packing and thus are important for protein stability and trafficking [22]. Because of the presumed role of R143 in protein stability we tested whether R143 might form an ion pair with the highly conserved residue D15, located at the cytosolic end of helix 1, or E369 at the cytosolic end of helix 10. The wild-type-like K_m and pH-dependence of the D15N mutation argues against a role of this residue in ion pair formation with R143. D15, nevertheless, appears to be important for protein trafficking, as suggested by its delayed surface expression. Moreover, trafficking defects are usually ameliorated in oocytes because of the low temperature used for oocyte storage (results not shown) and therefore it is likely that this mutant would not reach the plasma membrane when expressed in mammalian cells. The loss of activity in the E369R mutation further supports the important role of helix 10 in substrate transport [10,11]. The double mutation MCT1(R143E/E369R), however, did not rescue the transport defect. This experiment does not exclude an interaction between both residues but demonstrates that formation of a charge pair alone cannot explain the role of R143.

A second set of experiments suggests an involvement of R143 in conformational changes during transporter turnover. Our results indicate that V_{max} of acetate transport is identical in the R143H mutant and in the wild-type, whereas V_{max} of lactate was strongly reduced. MCT1 is prone to trans-stimulation, which indicates that the conformational change of the empty carrier is the slowest step of the transport cycle. As a result, V_{max} values of all substrates should be similar unless a different step is rate limiting. In the wild-type, V_{max} of acetate is considerably slower than V_{max} of lactate, suggesting that V_{max} of acetate is indeed governed by a different mechanism, possibly the release of the substrate. The decrease of lactate V_{max} combined with the lack of an effect on acetate V_{max} indicates that R143H reduces the velocity of the return of the empty carrier. The differences observed between acetate and lactate transport in MCT1 versus R143H cannot be explained by non-ionic diffusion of acetate. Acetate is permeable to non-injected oocytes and causes acidification of the cytosol. At an extracellular pH of 7.0 the acidification, however, is slow (about 0.02–0.03 pH units/min). As a result, the change of the pH_i caused by non-ionic diffusion will not exceed 0.1 pH unit during a 5 min uptake period. The most likely explanation is that helix 5 moves during the conformational change of the empty carrier, but may not directly participate in substrate translocation.

A third set of experiments suggested an involvement of residues R143H and K142Q in stereoselectivity. In the R143H mutant stereoselectivity was increased, whereas mutating K142 to glutamine decreased stereoselectivity. The effect is somewhat surprising because the loop between helix 4 and 5 is very likely to be localized intracellularly, whereas competition takes place on the exofacial side of the transporter. However, it has to be kept in mind that kinetic parameters of lactate transport are constrained by the Haldane relationship $(V_{max}/K_m)_{influx} = (V_{max}/K_m)_{efflux}$ [2]. As a result, changes of kinetic constants for influx affect kinetic constants of efflux. In agreement with this notion we found a reduced efflux velocity in the K142Q mutant. The relationship between MCT1 kinetic parameters is also exemplified by the triple mutant K137Q/K141Q/K142Q. The increased K_m of this

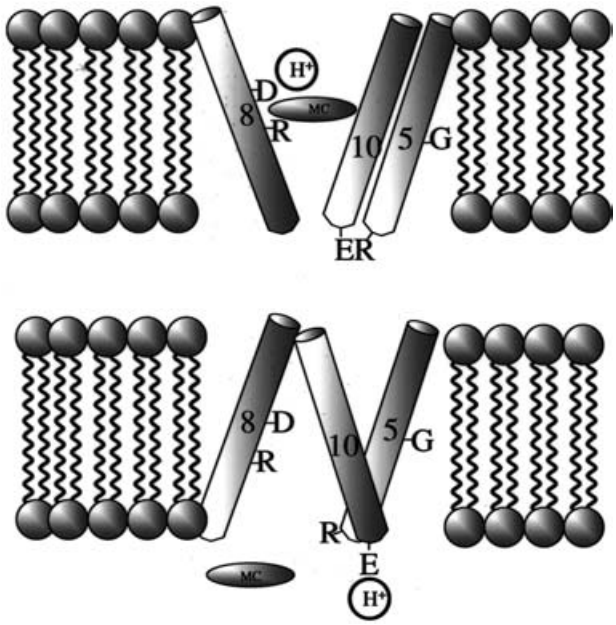

Figure 11 Hypothetic model of MCT1 transport function

Depicted are helices 5, 8 and 10, which contain residues that are essential for transport activity. R306 (R) in helix 8 is very likely involved in lactate binding. By exclusion of other residues it is proposed that D302 (D) and E369 (E) are involved in proton transport. Binding of monocarboxylates (MC, ellipsoid shape) to R306 may cause protons to move to E369, which disrupts a putative ion pair between E369 and R143. Lactate is released and the subsequent release of the proton initiates the return of the unloaded carrier to its original conformation, which involves movement of helix 5 (not depicted).

mutant is balanced by a similar increase of V_{max}, rendering the ratio V_{max}/K_m almost constant.

Analysis of site-specific mutants of MCT1 have so far revealed five essential residues, namely R143, G153 (both helix 5), D302, R306 (both helix 8) and E369 (helix 10). This has to be seen in comparison with thirteen other residues that have been mutated in this and other studies, without altering transport activity to a large extent. Particularly, we could not identify any residue in transmembrane helices (e.g. C106, C188, C189, C336, H337, E391; [10] and results not shown) that would alter proton translocation, which suggests that D302 and E369 might be involved in this function. Involvement of E369 in proton binding would also explain why transport was not rescued in the double mutant R143E/E369R. Helix 8 and helix 10 on the one hand appear to be involved in substrate translocation and, possibly, in proton translocation as proposed in a previous study [10]; helix 5 on the other hand is likely to undergo conformational changes during the transport cycle without being directly involved in substrate translocation. The loops between helices may serve as a filter region to select substrates. This is indicated by identification of DIDS binding residues in the loop TM7/TM8 and TM11/TM12 [12] and the altered stereoselectivity occurring through mutation of residues in the loop TM4/TM5.

The essential residues of MCT1 can be combined in a meaningful way to be in line with the kinetic mechanism of MCT1 (Figure 11). Protons are initially bound to D302. Lactate binding to R306 interferes with proton binding to D302 causing the proton to move to E369, which, in turn disrupts its interaction with R143, causing the helices to rearrange. Helix 5 would not move during substrate translocation but during reorientation of the transporter. The proposed mechanism partially resembles the well-characterized transport mechanism of another member of the multifacilitator superfamily, the lactose permease LacY, the structure of which has very recently been resolved [23]. LacY is a H^+-lactose cotransporter with the same binding order as MCT1. A comparison of both transporters indicates that D302 of MCT1 has a similar position to E269 of LacY, which is the proton acceptor site in the centre of helix 8. Secondly, substrate binding in LacY is incompatible with protonation of E269, causing the proton to move to a second acidic residue E325.

We thank Dr Pierre J. Magistretti for the gift of MCT1 antibodies. This study was funded by Australian Research Council Grant DP0208961 to S. B. and a Grant of the Deutsche Forschungsgemeinschaft to J. W. D. (De231/16-1).

REFERENCES

1 Halestrap, A. P. and Price, N. T. (1999) The proton-linked monocarboxylate transporter (MCT) family: structure, function and regulation. Biochem. J. **343**, 281–299
2 Halestrap, A. P. and Meredith, D. (2003) The SLC16 gene family – from monocarboxylate transporters (MCTs) to aromatic amino acid transporters and beyond. Pflugers Arch. Int., DOI: 10.1007/s00424-003-1067-2
3 Carpenter, L. and Halestrap, A. P. (1994) The kinetics, substrate and inhibitor specificity of the lactate transporter of Ehrlich–Lettre tumour cells studied with the intracellular pH indicator BCECF. Biochem. J. **304**, 751–760
4 Deuticke, B. (1982) Monocarboxylate transport in erythrocytes. J. Membr. Biol. **70**, 89–103
5 De Bruijne, A. W., Vreeburg, H. and Van Steveninck, J. (1983) Kinetic analysis of L-lactate transport in human erythrocytes via the monocarboxylate-specific carrier system. Biochim. Biophys. Acta **732**, 562–568
6 Broer, S., Rahman, B., Pellegri, G., Pellerin, L., Martin, J. L., Verleysdonk, S., Hamprecht, B. and Magistretti, P. J. (1997) Comparison of lactate transport in astroglial cells and monocarboxylate transporter 1 (MCT 1) expressing *Xenopus laevis* oocytes. Expression of two different monocarboxylate transporters in astroglial cells and neurons. J. Biol. Chem. **272**, 30096–30102
7 Broer, S., Schneider, H. P., Broer, A., Rahman, B., Hamprecht, B. and Deitmer, J. W. (1998) Characterization of the monocarboxylate transporter 1 expressed in *Xenopus laevis* oocytes by changes in cytosolic pH. Biochem. J. **333**, 167–174
8 Poole, R. C., Sansom, C. E. and Halestrap, A. P. (1996) Studies of the membrane topology of the rat erythrocyte H^+/lactate cotransporter (MCT1). Biochem. J. **320**, 817–824
9 Price, N. T., Jackson, V. N. and Halestrap, A. P. (1998) Cloning and sequencing of four new mammalian monocarboxylate transporter (MCT) homologues confirms the existence of a transporter family with an ancient past. Biochem. J. **329**, 321–328
10 Rahman, B., Schneider, H. P., Broer, A., Deitmer, J. W. and Broer, S. (1999) Helix 8 and helix 10 are involved in substrate recognition in the rat monocarboxylate transporter MCT1. Biochemistry **38**, 11577–11584
11 Garcia, C. K., Goldstein, J. L., Pathak, R. K., Anderson, R. G. and Brown, M. S. (1994) Molecular characterization of a membrane transporter for lactate, pyruvate, and other monocarboxylates: implications for the Cori cycle. Cell (Cambridge, Mass.) **76**, 865–873
12 Meredith, D., Roberts, M. and Halestrap, A. P. (1999) Both K290 and K413 are essential for DIDS covalent modification of the rat proton-linked monocabroxylate (lactate) transporter MCT1 expressed in *Xenopus laevis* oocytes. J. Physiol. **517P**, 25P
13 Broer, S., Broer, A., Schneider, H. P., Stegen, C., Halestrap, A. P. and Deitmer, J. W. (1999) Characterization of the high-affinity monocarboxylate transporter MCT2 in *Xenopus laevis* oocytes. Biochem. J. **341**, 529–535
14 Garcia, C. K., Brown, M. S., Pathak, R. K. and Goldstein, J. L. (1995) cDna cloning of Mct2, a second monocarboxylate transporter expressed in different cells than Mct1. J. Biol. Chem. **270**, 1843–1849
15 Broer, S. (2003) *Xenopus laevis* oocytes. in Membrane Transporters (Yan, Q., ed.), pp. 245–258, Humana Press, Totowa
16 Munsch, T. and Deitmer, J. W. (1994) Sodium bicarbonate cotransport current in identified leech glial cells. J. Physiol. (London) **474**, 43–53
17 Pierre, K., Pellerin, L., Debernardi, R., Riederer, B. M. and Magistretti, P. J. (2000) Cell-specific localization of monocarboxylate transporters, MCT1 and MCT2, in the adult mouse brain revealed by double immunohistochemical labeling and confocal microscopy. Neuroscience **100**, 617–627
18 Welter, K. (1981) Mathematik für Physiker, vol. 2, Friedrich Vieweg & Sohn, Braunschweig
19 Chillaron, J., Estevez, R., Samarzija, I., Waldegger, S., Testar, X., Lang, F., Zorzano, A., Busch, A. and Palacin, M. (1997) An intracellular trafficking defect in type I cystinuria rBAT mutants M467T and M467K. J. Biol. Chem. **272**, 9543–9549

20 Jung, K., Jung, H., Colacurcio, P. and Kaback, H. R. (1995) Role of glycine residues in the structure and function of lactose permease, an *Escherichia coli* membrane transport protein. Biochemistry **34**, 1030–1039
21 Wilson, M. C., Meredith, D. and Halestrap, A. P. (2002) Fluorescence resonance energy transfer studies on the interaction between the lactate transporter MCT1 and CD147 provide information on the topology and stoichiometry of the complex in situ. J. Biol. Chem. **277**, 3666–3672
22 Merickel, A., Kaback, H. R. and Edwards, R. H. (1997) Charged residues in transmembrane domains II and XI of a vesicular monoamine transporter form a charge pair that promotes high affinity substrate recognition. J. Biol. Chem. **272**, 5403–5408
23 Abramson, J., Smirnova, I., Kasho, V., Verner, G., Kaback, H. R. and Iwata, S. (2003) Structure and mechanism of the lactose permease of *Escherichia coli*. Science (Washington, D.C.) **301**, 610–615

Received 30 May 2003/14 August 2003; accepted 28 August 2003
Published as BJ Immediate Publication 28 August 2003, DOI 10.1042/BJ20030799